



Confidence Interval of Bayesian Network and Global Sensitivity Analysis

Sangjune Bae,* Nam H. Kim,† and Chanyoung Park‡
University of Florida, Gainesville, Florida 32611-6250

and
Zaeill Kim§

Agency for Defense Development, Daejeon 305-600, Republic of Korea

DOI: 10.2514/1.J055888

A Bayesian network represents a causal relationship among random variables using conditional probabilities. Because of limited resources and sampling uncertainty, the estimated probabilities have both aleatory randomness and epistemic uncertainty. In this paper, two approaches are used to estimate the confidence intervals of component- and system-level probabilities. The first approach uses an analytical method, where a normal distribution is assumed for the component- and system-level probabilities. Another approach is the bootstrap method, which uses resampling to build a distribution of the probabilities. Global sensitivity is analyzed as well to identify the component-level probability that most significantly affects the uncertainty in the system level. It is shown that the confidence intervals of system probability can be effectively narrowed by reducing sampling uncertainty in the most significant component.

Nomenclature

$A_{e,\text{tot}}$	=	sum of charge particle surface area
A_e^{surf}	=	surface area of heating element
A_{ps}	=	cross-sectional area of piston chamber
C_P	=	heat capacity
d_e	=	heating element diameter
e	=	burning distance
F_{ba}	=	frictional force of balls
F_{or}	=	frictional force of O-ring
F_{sh}	=	shearing force of shear pin
I	=	input current
I_F	=	indicator function
h	=	subfunction by analysis of variance decomposition
l_e	=	heating element length
l_{pin}	=	length of pin
m	=	total number of component-level probability of failure
m_{ba}	=	mass of ball
m_c	=	mass of charge
m_{ps}	=	mass of piston
n	=	total number of samples
P	=	heating rate of heating element
P_F	=	probability of failure
P_F^i	=	i th conditional probability of failure
P_F^{sys}	=	system probability of failure
P_{ps}	=	chamber pressure
Q_{loss}	=	heat transfer
R	=	resistance of heating element
R_g	=	universal gas constant
r_b	=	burning rate
r_{ba}	=	radius of ball
r_w	=	resistivity of heating element

T	=	temperature of heating element
T_g	=	gas flame temperature
T_{pin}	=	temperature at the end of pin
T_0	=	ambient temperature
V_{ps}	=	piston chamber volume
\mathbf{x}_i	=	i th input random vector
$x_{i,j}$	=	i th input random variable of the j th component
y_i	=	i th output of a component
$y_{i,\text{th}}$	=	threshold value of the i th conditional probability
γ	=	ratio of specific heats
ε	=	emissivity
η_p	=	correction factor
κ	=	conductivity of heating element
μ_c	=	mean of component probability of failure
v_{ps}	=	velocity of piston
ρ_c	=	density of charge
σ	=	Stefan–Boltzmann constant
$\sigma_{c,\text{sys}}$	=	standard deviation of component probability of failure
σ_F	=	standard deviation of system probability of failure

I. Introduction

IN THE early design stage, engineers need to estimate the safety of their design by calculating the system probability of failure. When a system is composed of many components, engineers should understand the structure of the system as well as how the component probability of failure propagates to the system. In this paper, the system probability of failure means the probability of failure at the system level. In some literature, system probability of failure also means the probability of multiple failure modes, which is different usage from this paper [1].

One way to represent the component–system relationship is a Bayesian network [2,3], which is also known as a belief network. A Bayesian network represents the probabilistic relationships of a set of components in a hierarchical information graph, which is called a directed acyclic graph (DAG), whose detailed explanation will be provided in Sec. II. This network is useful to understand how a component probability of failure propagates through the network and how significantly it affects the system probability of failure.

The probability in a Bayesian network is induced from two different sources of uncertainty: aleatory randomness and epistemic uncertainty [4]. The aleatory randomness comes from the natural variability of input and is irreducible; the randomness is usually modeled through a probability density function. On the other hand, epistemic uncertainty is originated from the lack of knowledge or

Received 1 December 2016; revision received 13 April 2017; accepted for publication 14 April 2017; published online 29 June 2017. Copyright © 2017 by Nam Ho Kim. Published by the American Institute of Aeronautics and Astronautics, Inc., with permission. All requests for copying and permission to reprint should be submitted to CCC at www.copyright.com; employ the ISSN 0001-1452 (print) or 1533-385X (online) to initiate your request. See also AIAA Rights and Permissions www.aiaa.org/randp.

*Graduate Student, Department of Mechanical Engineering, P.O. Box 116250.

†Professor, Department of Mechanical Engineering, P.O. Box 116250, Associate Fellow AIAA.

‡Research Scientist, Department of Mechanical Engineering, Member AIAA.

§Senior Researcher, Yuseong, P.O. Box 35.

limited data, which can be reduced by improving knowledge or allocating more resources.

When a set of samples are used to calculate the probability of failure at a component level, there exist both aleatory randomness and epistemic uncertainty. These uncertainties directly affect the output of the component and are propagated through the network to cause uncertainty in system performance. In this paper, it is assumed that the probability of failure of a component is determined through a sampling method, such as Monte Carlo simulation. In such a case, the estimated probability of failure has sampling uncertainty due to the finite number of samples, which is the only epistemic uncertainty considered in this paper. If different methods are used to estimate the probability of failure, such as the first-order reliability method, then the approximation error can be accounted for epistemic uncertainty. When a quantity of interest has epistemic uncertainty, it is important to estimate the confidence interval to make a reliable decision.

Although the confidence interval of a system reliability has been of high interest for decades [5–7], not much work has been done thus far regarding the confidence interval of a system that is defined as a Bayesian network. In the traditional reliability assessment, only the system-level reliability has been the focus. However, a success in a system does not guarantee all components' success, and vice versa [8]. A Bayesian network can manage this lack of connection between the system and the components. Regarding a Bayesian network, Cheng and Druzdzel used two sampling algorithms, so-called he AIS-BN- μ and AIS-BN- σ algorithms, to calculate the probability of failure of a Bayesian network within prescribed precision focusing on the convergence of the importance distribution [9].

Although conventional reliability methods can calculate the system reliability as well as its confidence intervals, this paper focuses on identifying the contribution of component-level reliability and confidence intervals to that of system. For this purpose, the Bayesian network provides a unique framework to facilitate the relationship between components and the system. Different from previous studies, this paper addresses how to estimate the confidence interval of an individual component probability of failure as well as the system probability using two different methods. Further, global sensitivity analysis will be introduced to identify important components whose epistemic uncertainty significantly contributes to the system's epistemic uncertainty and to efficiently reduce the system's confidence interval to make a conservative decision by controlling sampling uncertainty.

The paper is organized as follows. Section II introduces several methods of estimating the confidence interval of the system that is represented using a Bayesian network. Section III presents the global sensitivity analysis to evaluate the contribution of the uncertainty in the component level to the uncertainty in the system level. In Sec. IV, confidence intervals using different methods are compared using an analytical example. Section V shows a Bayesian network example of pyromechanical devices with confidence interval and sensitivity analysis results. Section VI presents conclusions with a suggestion of possible methods under different conditions.

II. Confidence Interval of Bayesian Network

The objective of this section is to find the confidence interval of a component and of the system. Figure 1 shows an example of a Bayesian network. The Bayesian network is represented by a graphical model, called directed acyclic graph (DAG), and probability tables associated with it. The graphical model consists of nodes and arrows. The nodes are depicted by the circles on Fig. 1, and they represent components in the system. The arrows connecting the nodes are called causal edges, and these edges show how a node affects others. The node from which a causal edge starts is called “parent node”, and the node that receives the causal edge is called “child node”. A child node is conditioned on a parent node, and in some cases, there can be more than two parent nodes, as node C in Fig. 1.

On either side of a node, there is a table describing the probability of failure of the node, conditioned on its parent nodes. For example, node D is conditioned on node C. Therefore, there are two possible failures that can occur in node D; node D fails when node C succeeds, and node D fails when node C fails. The table, therefore, calculates each conditional probability of failure. Then, the Bayesian network allows calculating the system probability of failure by considering all possible scenarios [10].

In this paper, it is assumed that the probabilities are calculated using a sampling method (e.g., Monte Carlo simulation). Because of the finite number of samples, the calculated probabilities have sampling uncertainty. Therefore, to be conservative in estimating probabilities, it is necessary to estimate the confidence intervals. For a single component, the confidence intervals can be calculated by estimating sampling uncertainty [11]. However, when a system is composed of many components using DAG, estimating the confidence intervals of system performance can be non-trivial, which is the objective of the paper.

Figure 1 also shows an example of a sampling-based method of calculating the probability of failure of a component. In this case, component A has k input random variables with n number of samples from each random variable. In the figure, $x_{i,j}$ ($i = 1, \dots, n; j = 1, \dots, k$) represents the i th sample of the j th random variable for component A; x_i represents the i th vector of samples from all random variables; and y_i represents the i th output of component A from sample x_i . Each component may have different numbers of random variables and samples; therefore, the size and the number of the random sample vector can vary.

The term “component confidence interval” (CCI) is used to represent a confidence interval of the probability of failure of a component, whereas “system confidence interval” (SCI) represents that of the entire Bayesian network under consideration. These terms are often used hereinafter to describe such intervals.

Two different methods are presented to build a confidence interval: the interval method and bootstrap method. The interval method assumes that the output distribution of a component follows a binomial distribution with unknown probability of failure, where analytical solutions are provided with different approaches to building a confidence interval. The bootstrap method uses

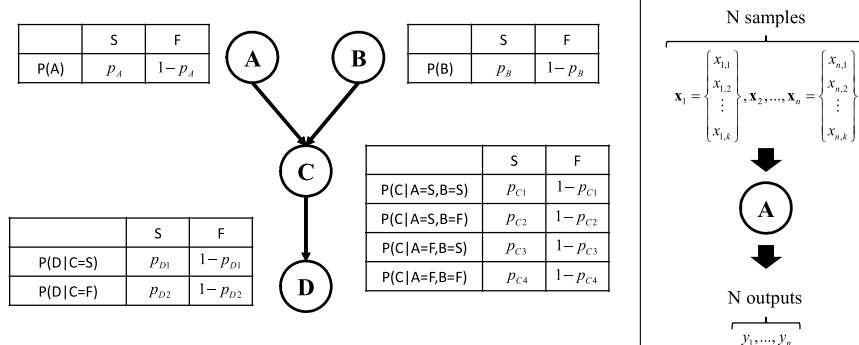


Fig. 1 Example of Bayesian network and sampling-based method of calculating probability of failure.

resampling to find an empirical distribution of the output, from which the desired percentile value is calculated as the bounds of the confidence interval.

A. Component-Level Interval Estimation

When n number samples of output, y_i ($i = 1, \dots, n$), are available, the probability of failure (P_F) of the component can be defined as the sum of indicator functions over the total number of samples as

$$P_F = \frac{1}{n} \sum_{i=1}^n I_F(y_i) \tag{1}$$

where the indicator function becomes 1 if y_i belongs to the failure region F ; otherwise 0, as

$$I_F(y_i) = \begin{cases} y_i & \text{if } y_i \in F \\ 0 & \text{if } y_i \notin F \end{cases} \tag{2}$$

The summation of the indicator function nP_F follows a binomial distribution $B(n, P_F)$ because it satisfies the following necessary conditions [12].

- 1) The number of observations n is fixed.
- 2) Each observation is independent.
- 3) Each observation represents one of two outcomes (“success” or “failure”).
- 4) The probability of failure P_F is the same for each outcome.

Condition 4 is valid because both y_{th} and the distribution of y_i are assumed to be fixed; the variability is only due to the aleatory sampling randomness.

The simplest way to build a CCI is using a normal approximation. When n is sufficiently large, the distribution of P_F can be estimated by a normal distribution with the mean $\mu = \hat{P}_F$ and the standard deviation σ_F by the central limit theorem. Brown et al. claimed that n must be large enough so that both $n\hat{P}_F$ and $n(1 - \hat{P}_F)$ are larger than 10 to be approximated as a normal distribution [13]. The standard deviation of P_F can be estimated as

$$\hat{\sigma}_F = \sqrt{\frac{\hat{P}_F(1 - \hat{P}_F)}{n}} \tag{3}$$

In this paper, the circumflex accent hereinafter represents an estimate of the statistics. If the normality assumption holds, then the confidence interval of P_F (or so-called “Wald” confidence interval) is provided as

$$\left[\hat{P}_F - z_{1-\alpha/2} \sqrt{\frac{\hat{P}_F(1 - \hat{P}_F)}{n}}, \hat{P}_F + z_{1-\alpha/2} \sqrt{\frac{\hat{P}_F(1 - \hat{P}_F)}{n}} \right] \tag{4}$$

where $z_{1-\alpha/2}$ is the z -score, and $1 - \alpha$ is the corresponding confidence level. If the number of samples is insufficient, however, this normality assumption is no longer valid. This normality approximation has two problems [14]. First, if P_F is near 0 or 1, then $\sigma_F \approx 0$. Thus, it underestimates the uncertainty in P_F . Second, the confidence interval based on a normal distribution approximation has a domain of $[-\infty, \infty]$, which easily exceeds the domain of P_F , $[0, 1]$. To compensate for domain exceedance, Wilson [15] developed a CCI based on inverting the z -test, which may apply even for a small number of samples or a very small probability. The lower and upper limits of the confidence interval are estimated as the roots of $|p - \hat{P}_F| = z_{1-\alpha/2} \sqrt{p(1-p)/n}$.

Lower limit:

$$\left(\hat{P}_F + \frac{z_{1-\alpha/2}^2}{2n} - z_{1-\alpha/2} \sqrt{\frac{\hat{P}_F(1 - \hat{P}_F)}{n} + \frac{z_{1-\alpha/2}^2}{4n^2}} \right) / \left(1 + \frac{z_{1-\alpha/2}^2}{n} \right) \tag{5a}$$

Upper limit:

$$\left(\hat{P}_F + \frac{z_{1-\alpha/2}^2}{2n} + z_{1-\alpha/2} \sqrt{\frac{\hat{P}_F(1 - \hat{P}_F)}{n} + \frac{z_{1-\alpha/2}^2}{4n^2}} \right) / \left(1 + \frac{z_{1-\alpha/2}^2}{n} \right) \tag{5b}$$

On the other hand, Clopper and Pearson proposed an exact confidence interval [16]. The confidence interval can be obtained by solving the following equation sets using the beta distribution [17]:

$$\begin{aligned} \sum_{x=0}^{n_f} \binom{n}{x} p_U^x (1 - p_U)^{n-x} &= \frac{\alpha}{2} \\ \sum_{x=n_f}^n \binom{n}{x} p_L^x (1 - p_L)^{n-x} &= \frac{\alpha}{2} \end{aligned} \tag{6}$$

By introducing F -distribution, it is possible to approximate the confidence interval as

$$\left[\frac{n_f}{n_f + (n - n_f + 1)F_{1-\alpha/2; 2n_f, 2(n-n_f+1)}}, \frac{(n_f + 1)F_{1-\alpha/2; 2(n-n_f+1), 2(n-n_f)}}{(n - n_f) + (n_f + 1)F_{1-\alpha/2; 2(n_f+1), 2(n-n_f)}} \right] \tag{7}$$

Although the word “exact” has been used, this is still an approximation of the true confidence interval because a binomial distribution is discrete, whereas F -distribution is continuous. More recently, Sauro and Lewis [18] showed that the adjusted Wald method works well for building a CCI with a small number of samples. The formula is proposed as

$$\left[\hat{P}_{adj} - z_{1-\alpha/2} \sqrt{\frac{\hat{P}_{adj}(1 - \hat{P}_{adj})}{n_{adj}}}, \hat{P}_{adj} + z_{1-\alpha/2} \sqrt{\frac{\hat{P}_{adj}(1 - \hat{P}_{adj})}{n_{adj}}} \right] \tag{8}$$

where $\hat{P}_{adj} = (n\hat{P}_F + z_{1-\alpha/2}^2/2)/(n + z_{1-\alpha/2}^2)$, and $n_{adj} = n + z_{1-\alpha/2}^2$. The CCI can be estimated using one of the four methods described previously.

B. System-Level Interval Estimation

Although the component-level interval methods in the previous section can be used to build a CCI, they cannot be used to build a confidence interval for the system. The DAG in a Bayesian network explains the relationship among the components, which makes it possible to express the SCI as a function of P_F^i . In Bayesian network, the probability of failure (P_F^i) of the i th component is, in fact, the conditional P_F , given its parent nodes. The system P_F is provided as an explicit form by DAG. However, propagating the confidence interval of each component to obtain the confidence level of the system is difficult in classical statistics [19]; that is, calculating an analytical distribution of a function of random variables is mathematically challenging. Instead, in this paper, the mean and variance of the system P_F are estimated as

$$E[P_F^{sys}] = P_F^{sys}(\hat{P}_F^1, \hat{P}_F^2, \dots, \hat{P}_F^k) \tag{9}$$

$$V[P_F^{sys}] = E[(P_F^{sys})^2] - E[P_F^{sys}]^2 \tag{10}$$

That is, the mean of the system P_F is estimated using the means of component P_F , whereas the variance is the mean of the square minus the square of the mean. In Eq. (10), the variance of the system P_F

Table 1 Mean and standard deviation estimated from different methods

Method	Mean ($\mu_{c,i}$)	Standard deviation ($\sigma_{c,i}$)
Wald	\hat{P}_F^i	$\sqrt{(\hat{P}_F^i(1 - \hat{P}_F^i)/n)}$
Wilson	$(\hat{P}_F^i + z_{1-\alpha/2}^2/2n)/(1 + z_{1-\alpha/2}^2/n)$	$\sqrt{(\hat{P}_F^i(1 - \hat{P}_F^i)/n + (z_{\alpha/2}^2/4n^2))/(1 + (z_{\alpha/2}^2/n))}$
Adjusted Wald	\hat{P}_{adj}^i	$\sqrt{(\hat{P}_{adj}^i(1 - \hat{P}_{adj}^i)/n_{adj})}$

depends on both the mean and variance of component P_F because P_F^{sys} is an uncertain variable that depends on the mean and variance of component P_F through the Bayesian network.

Equations (9) and (10) can be calculated analytically through a Bayesian network. In the case of a component, the CCI can be defined in the form of $\mu_{c,i} \pm z_{1-\alpha/2}\sigma_{c,i}$, where $\mu_{c,i}$ and $\sigma_{c,i}$ are, respectively, the mean and standard deviation of the component P_F . For Wald, Wilson, and adjusted Wald methods, the mean and standard deviations are listed in Table 1. The same idea can be used to calculate an SCI by employing the mean and variance of the system given in Eqs. (9) and (10). The mean of system probability of failure (\hat{P}_F^{sys}) is estimated by substituting Eq. (9) with the mean of each component, whereas the standard deviation of system P_F ($\hat{\sigma}_F^{sys}$) can be obtained by applying Eq. (10). Once the mean and standard deviation of system P_F are available, the SCI can be written as

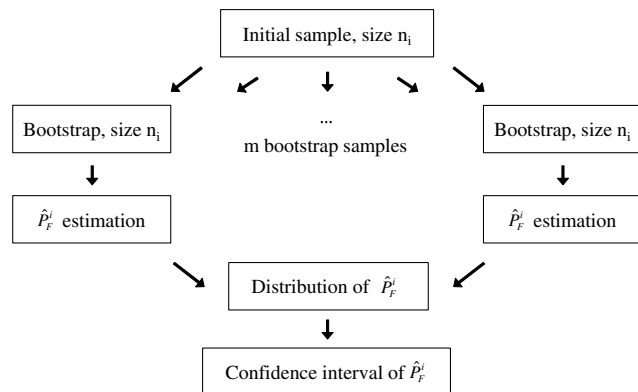
$$\left[\hat{P}_F^{sys}(\boldsymbol{\mu}_c) - z_{1-\alpha/2}\hat{\sigma}_F^{sys}(\hat{P}_F^{sys}(\boldsymbol{\mu}_c)), \hat{P}_F^{sys}(\boldsymbol{\mu}_c) + z_{1-\alpha/2}\hat{\sigma}_F^{sys}(\hat{P}_F^{sys}(\boldsymbol{\mu}_c)) \right] \quad (11)$$

where $\boldsymbol{\mu}_c = \{\mu_{c,1}, \mu_{c,2}, \dots, \mu_{c,k}\}$ is the vector of estimated component probabilities of failure, and $\hat{\sigma}_F^{sys}(\hat{P}_F^{sys}(\boldsymbol{\mu}_c))$ is the square root of the variance in Eq. (10).

C. Bootstrap Method

Resampling methods can play a significant role in finding a distribution of the statistic of interest, and the bootstrap method is one of them [20]. The bootstrap method generates pseudosample sets by random sampling with replacement from the initial samples. There are two bootstrap methods: nonparametric and parametric.

The nonparametric bootstrap method is used when the underlying distribution of the samples is unknown. Figure 2 illustrates the nonparametric bootstrap method. When n_i number of output samples, which are also called the initial sample set hereinafter, are provided for a component, a nonparametric bootstrap sample set can be obtained through resampling with replacement without assuming any distribution type for the sample set. That is, a sample is randomly chosen out of the initial samples, and it is replaced. This procedure is repeated n_i times, which is the equal number of the initial sample set, to establish a set of pseudosamples, which is called a bootstrap sample set. Using a bootstrap sample set, the statistic of interest can be estimated. This procedure is repeated for m times, where m is a

**Fig. 2** Procedure of nonparametric bootstrap method.

desired number of repetition. The empirical distribution of the statistic of interest can be found with m number of estimates.

On the other hand, the parametric bootstrap method is used when the underlying output distribution is known or assumed. When the output of a component follows a specific distribution, the bootstrap sample sets are generated repeatedly from the distribution. Then, the statistic of interest is estimated from each sample set, allowing the statistics to form an empirical distribution.

As mentioned earlier, if the initial data set does not satisfy $n\hat{P}_F > 10$ and $n(1 - \hat{P}_F) > 10$ so that normal distribution approximation is not justified, the nonparametric bootstrap method will be used in this paper. The statistic of interest is the component P_F . Using the nonparametric bootstrap method, the distribution of \hat{P}_F^i is generated by repetition. Here, the true P_F is estimated through the distribution. Last, a CCI is constructed by taking $\alpha/2$ and $1 - \alpha/2$ percentile values of the distribution as the lower and upper bounds of the confidence interval where $1 - \alpha$ is the corresponding confidence level.

The system P_F can be calculated by substituting the component probabilities of failure in Eq. (9) with an estimate obtained from each bootstrap sample set. As in the component level, the distribution of the system P_F can also be obtained by repeating this process. The mean is estimated through the distribution, and finally, a SCI with the $(1 - \alpha)\%$ confidence level is built up by taking $\alpha/2$ and $1 - \alpha/2$ percentile values of the distribution.

III. Global Sensitivity Analysis

Although the SCI can be obtained through different methods introduced in Sec. II, the outcome may not be useful if the SCI is too wide for a given design. When the estimated system P_F has a confidence interval, a conservative design has to be used to compensate for it. In the conventional reliability-based design, a conservative design is obtained that can compensate for either aleatory uncertainty only [21] or both aleatory and epistemic uncertainty [22,23]. When the SCI is too large, however, the design becomes too conservative and may not be useful for practice.

Because the SCI in this paper is caused by sampling uncertainty of components (i.e., CCIs), and because the CCIs are inversely proportional to the number of samples as shown in Sec. II, it is important to understand the effect of the number of samples on the SCI. That is, it is important to understand how many samples should be added to a component to reduce the SCI most effectively. In this section, the global sensitivity analysis is performed to estimate the significance of individual CCIs on the SCI such that the SCI can be effectively reduced. In this paper, individual CCIs are represented by using the variance of the component P_F , which is controlled by the number of samples used for evaluating the P_F . It is noted that the expected value of the system P_F will not be varied, but only the SCI is.

A schematic diagram for the effect of the variance on a component level is illustrated in Fig. 3. In the figure, both systems have the same expected P_F : that is, $E[p_1^{sys}] = E[p_2^{sys}]$, but $V[p_1^{sys}]$ is larger than $V[p_2^{sys}]$. An important question on uncertainty management of a system is: to which component should more samples be provided to reduce the SCI most efficiently? To answer this question, global sensitivity analysis can be used.

Global sensitivity analysis, as the name implies, estimates the change of output as input variables vary over their entire domain. Therefore, it is possible to figure out how the uncertainty of output can be attributed to different uncertainty sources [24]. To perform

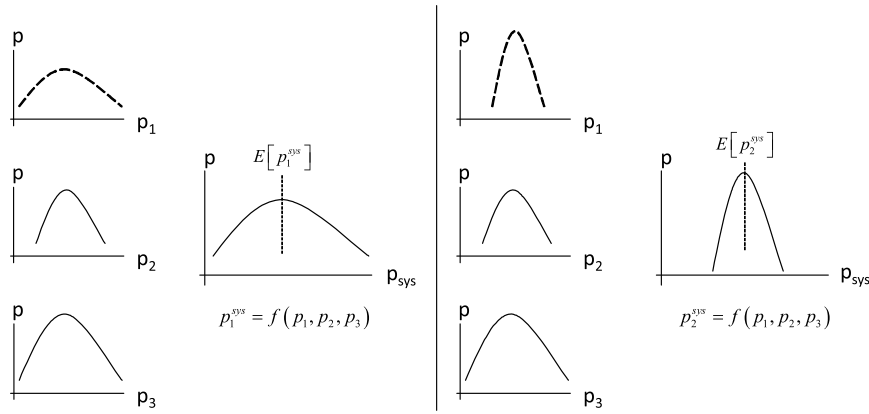


Fig. 3 Effect of variance of component probability of failure on system probability of failure.

global sensitivity analysis, analysis of variance (ANOVA) decomposition is used. ANOVA decomposition is a method of decomposing a function into subfunctions, which makes it possible to decompose the variance of output into the main effect and interaction effect. The main effect refers to the influence of a variable itself on the output variance, whereas the interaction effect reflects the influence of the interaction among multiple variables on the output variance.

A system probability of failure P_F^{sys} is a function of the component probability of failures $\mathbf{P}_F = \{P_F^1, P_F^2, \dots, P_F^m\}$, where m is the number of the component probability of failures. Because of sampling uncertainty, the component P_F has uncertainty, whose probability density function is defined as $q(P_F^i)$. Let $h(\mathbf{P}_F)$ denote a system P_F ; then, the system P_F can be decomposed into the summation of subfunctions $h(\mathbf{P}_F)$ as

$$h(\mathbf{P}_F) = h_0 + \sum_i h_i + \sum_{j>i} h_{ij} + \dots + h_{12\dots m} \quad (12)$$

where $h_i = h_i(P_F^i)$ is a subfunction related to the i th component-level probability; $h_{ij} = h_{ij}(P_F^i, P_F^j)$ is a subfunction related to two component-level probabilities, etc.; and the first term, h_0 , represents the constant term. The subfunctions in Eq. (12) can be calculated as

$$h_0 = \int_0^1 h(\mathbf{P}_F) \prod_i q(P_F^i) dP_F^i \quad (13)$$

$$h_{ij,\dots,r} = \int_0^1 h(\mathbf{P}_F) \prod_{k \neq i,j,\dots,r} q(P_F^k) dP_F^k - \sum_{k=i,j,\dots,r} h_k - \sum_{k=i,j,\dots,r} \sum_{l>k,l=i,j,\dots,r} h_{kl} - \dots - h_0 \quad (14)$$

The preceding decomposition allows the summation of the variance of each subfunction to be equal to the output variance. In other words, the output variance can be not only stated as a sum of fractional variance but also decomposed into main effect and interaction effect. The decomposition is shown as follows:

$$V[h(\mathbf{P}_F)] = \sum_i V[h_i] + \sum_{j>i} V[h_{ij}] + \dots + V[h_{12\dots m}] \quad (15)$$

Each term in Eq. (15) can be calculated as

$$V[h(\mathbf{P}_F)] = \int_0^1 h^2(\mathbf{P}_F) \prod_k q(P_F^k) dP_F^k - h_0^2 \quad (16)$$

$$V[h_{ij,\dots,r}] = \int_0^1 h_{ij,\dots,r}^2 \prod_{k=i,j,\dots,r} q(P_F^k) dP_F^k - h_0^2 \quad (17)$$

The global sensitivity index is defined as the ratio of fractional variance to the output variance. A sensitivity index with a single subscript is called “main sensitivity index”, and the one with more than two subscripts is called “interaction sensitivity index”:

$$S_{ij,\dots,r} = \frac{V[h_{ij,\dots,r}]}{V[h(\mathbf{P}_F)]} \quad (18)$$

To figure out which variable affects the output variance the most, both the main and interaction sensitivity index must be considered. Therefore, another index, called “total sensitivity index”, is defined to compare the effect of the variables:

$$S_{Ti} = S_i + S_{\sim i} \quad (19)$$

where $S_{\sim i}$ is the summation of all interaction sensitivity indices of which subscript includes i .

IV. Confidence Interval in Component Level

A single component example is provided to manifest how the CCIs obtained from the four interval methods and the bootstrap method behave differently. The interval methods are tested with different levels of P_F by gradually increasing the threshold value.

A. Comparison of Interval Methods for a Single Component

Consider a single component whose output y follows a normal distribution, and the P_F is determined based on a threshold y_{th} :

$$y \sim N(15.8, 5^2), \quad P_F = P(y \leq y_{\text{th}}) \quad (20)$$

When $y_{\text{th}} = 20$, the true P_F is 0.8. It is assumed that 1000 samples are employed to estimate the P_F for each component, assuming the true P_F is unknown. The estimated probability using 1000 samples is 0.792. In Table 2, the confidence intervals estimated using the four methods are compared at the 95% confidence level. A distribution made up of the 10,000 repetitions of probability calculation is assumed to be the true distribution of probability.

Among the four methods, the most conservative confidence interval (i.e., the widest interval) results from Wilson method, whereas the adjusted Wald and Wald method show a comparable size of the confidence interval. However, when compared to the true

Table 2 Comparison of confidence intervals

Method	Lower bound (A)	Upper bound (B)	Interval width (B-A)
True	0.7780	0.8200	0.0420
Wald	0.7663	0.8177	0.0514
Wilson	0.7411	0.8406	0.0995
Clopper–Pearson	0.7655	0.8467	0.0812
Adjusted Wald	0.7657	0.8160	0.0503

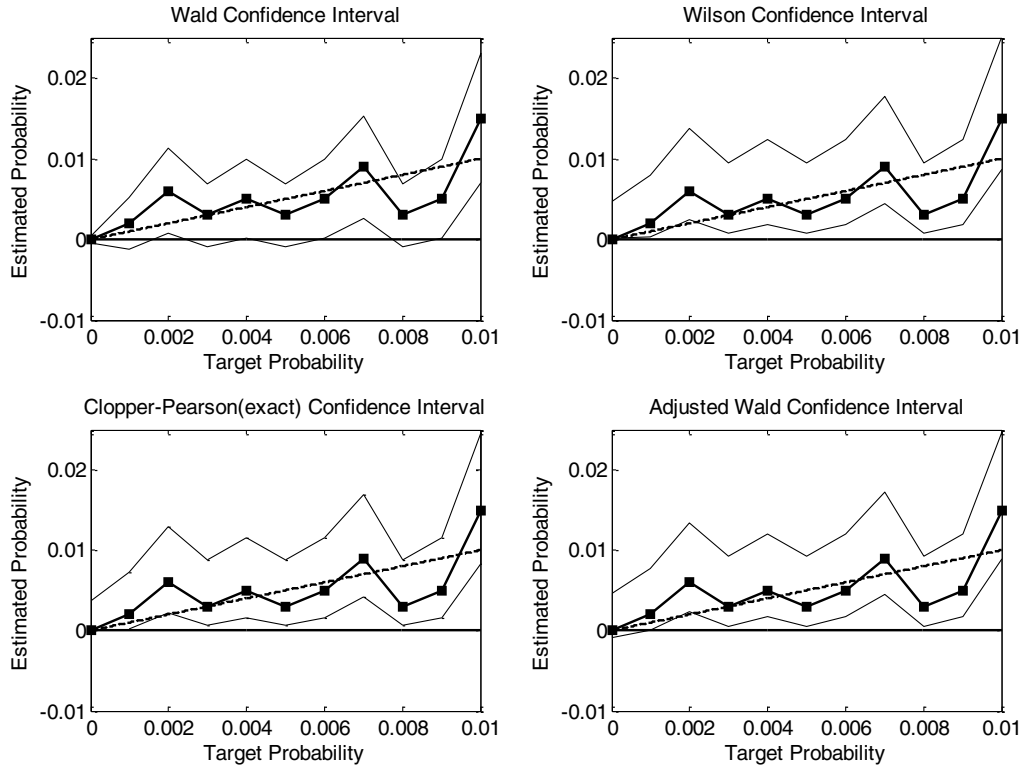


Fig. 4 Confidence interval estimation for high probability of failure.

distribution of probability, all four methods yield a conservative confidence interval; that is, the estimated interval is larger than the true one. It is also apparent that the Wald confidence interval is the only symmetric interval with respect to the sample P_F .

Because most engineering systems require a small value of P_F , it would be interesting to study the confidence interval in an extreme P_F , which is shown in Fig. 4. The threshold y_{th} in Eq. (20) is gradually decreased so that the P_F approaches zero. One thousand samples are used to calculate a CCI while the true P_F varies from 0.0 to 1.0%, in the increment of 0.1%. In Fig. 4, the dashed curve represents the true P_F , and the piecewise linear solid line represents estimated P_F . As previously discussed in Sec. II, the Wald and adjusted Wald methods resulted in a confidence interval exceeding the lower limit of probability, which is [0,1]. Wilson and Clopper-Pearson (exact) confidence intervals do not go below zero, although the interval width was wide compared to the Wald and adjusted Wald methods, as in Table 2.

B. Bootstrap Method for Confidence Interval Estimation

Using the same analytical example as in the previous section, it is investigated how the nonparametric bootstrap method predicts a confidence interval. Note that the initial data set contains 1000 values of either 0 or 1 by the indicator function in Eq. (2). As explained in Fig. 3, it takes as many as the initial data set to obtain one bootstrap sample set, which in this case is equal to 1000. Therefore, to obtain m repetitions, $1000 \times m$ number of resampling is needed.

First, the number of samples in the initial data set is fixed as 1000, and the number of repetition is varied to 100, 500, and 1000 to see the effect of bootstrap repetitions, as listed in Table 3. It is noted that generating initial samples is expensive because each sample requires a computer simulation or solving partial differential equation, whereas bootstrap repetition is not expensive because it is simply taking samples from the existing samples. However, it might be informative to test how many bootstrap repetitions are enough. The effect of the initial data set is also observed by fixing the number of bootstrap repetitions to 1000 while varying the number of initial data set to 100, 500, and 1000, as listed in Table 4. The 95% confidence level is employed in this example. As shown in Tables 3 and 4, the number of repetitions does not affect the standard deviation or confidence interval width. It is found that a confidence interval

estimation largely depends on the number of the initial data set. In other words, adding more repetition does not influence the interval width, whereas adding more initial data yields a narrower interval width. Thus, the number of repetitions becomes a minor concern as long as it is sufficient enough. Still, the question regarding how many repetitions are enough should be discussed in the future research.

V. Bayesian Network of Pyrotechnic Mechanical Device

A. Problem Definition

A pyrotechnic mechanical device (PMD) refers to a broad family of devices using chemical reaction to initiate mechanical operation. It is widely used in industry and military, such as airbag, rocket launch, and missile release, where a high-speed activation is required [25,26]. This disposable device is initiated by a chain of electrical, chemical, and mechanical functions. Because of its high importance, P_F must be maintained at a very low level. An example of PMD is illustrated in

Table 3 Effect of repetition on confidence interval estimation

Initial samples	1000	1000	1000
Bootstrap repetitions	100	500	1000
Mean estimate	0.793	0.791	0.791
Standard deviation	0.013	0.012	0.012
Lower bound (A)	0.767	0.765	0.767
Upper bound (B)	0.822	0.815	0.816
Interval width (B-A)	0.055	0.050	0.049

Table 4 Effect of initial data set on CCI estimation

Initial samples	100	500	1000
Bootstrap repetitions	1000	1000	1000
Mean estimate	0.82	0.80	0.791
Standard deviation	0.03	0.02	0.012
Lower bound (A)	0.70	0.76	0.767
Upper bound (B)	0.77	0.81	0.816
Interval width (B-A)	0.07	0.05	0.049

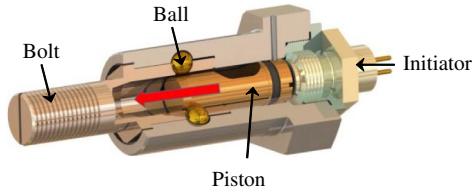


Fig. 5 Pyrotechnic mechanical device to release a bolt.

Fig. 5, where the pressure generated by expanding gas pushes the piston and releases the bolt. The PMD mainly consists of two parts that are serially connected, called the initiator and the pyrolock. When the initiator receives an electric signal, the temperature of the heating element goes up due to the applied current. The performance of the initiator is considered a success when the temperature of the heating element exceeds a threshold temperature to start a chemical reaction within 10 ms. Once initiated, the chemical reaction generates pressure, pushes the piston in the pyrolock, and releases the bolt. The system is considered a success if the piston moves enough such that the locking balls are dropped and the bolt is released.

The rate of temperature rise in the heating element is described by the following equations:

$$\frac{dT}{dt} = \frac{P(T)}{C_p} = \frac{1}{C_p} \left[I^2 R(T) - \frac{\pi \kappa d_e^2 (T - T_{\text{pin}})}{2l_{\text{pin}}} - \epsilon \sigma A_e^{\text{surf}} (T^4 - T_0^4) \right] \quad (21)$$

$$R(T) = 0.0005 \frac{l_e}{d_e^2} r_w(T) \quad (22)$$

$$r_w(T) = 70.604 + 0.06984T \quad (23)$$

where $R(T)$ is the temperature-dependent resistance, and $r_w(T)$ is the resistivity of the heating element. All other variables are explained in the Nomenclature. Detailed explanations of the model can be found by Jang et al. [25] and Hwang et al. [26].

The pyrolock starts working due to the pressure generated by the initiator; its behavior is analyzed through three different stages, in which a system of ordinary differential equations are employed. In stage 1, the piston does not move, but the pressure must be large enough to break the shear pin to proceed to the next stage. In stage 2, once the shear pin is broken, the piston starts moving if the pressure force is larger than the friction forces from the O-ring and balls. This stage continues until the balls are detached from the piston. Last, stage 3 explains the motion of the piston from the moment that the balls are detached from the piston to the complete separation of the bolt. The system is governed by the following differential equations [25,26]:

$$\frac{d\rho_c}{dt} = \frac{1}{V_{\text{ps}}} \left\{ \frac{dm_c}{dt} - \rho_c (A_{c,\text{tot}} r_b + A_{\text{ps}} v_{\text{ps}}) \right\} \quad (24)$$

$$\frac{dP_{\text{ps}}}{dt} = \frac{1}{V_{\text{ps}}} \left\{ \eta_p \frac{dm_c}{dt} R_g \gamma T_g - (\gamma - 1) \left(P_{\text{ps}} A_{\text{ps}} v_{\text{ps}} + \frac{dQ_{\text{loss}}}{dt} \right) - P_{\text{ps}} \frac{dV_{\text{ps}}}{dt} \right\} \quad (25)$$

$$\frac{dV_{\text{ps}}}{dt} = A_{c,\text{tot}} r_b + A_{\text{ps}} v_{\text{ps}} \quad (26)$$

$$\frac{de}{dt} = r_b \quad (27)$$

$$\frac{dv_{\text{ps}}}{dt} = \begin{cases} 0 & \text{(stage 1)} \\ \frac{P_{\text{ps}} A_{\text{ps}} - F_{\text{or}} - F_{\text{ba}}}{m_{\text{ps}}} & \text{(stage 2)} \\ \frac{P_{\text{ps}} A_{\text{ps}} - F_{\text{or}}}{m_{\text{ps}}} & \text{(stage 3)} \end{cases} \quad (28)$$

$$F_{\text{sh}} = \begin{cases} 234 & \text{(stage 1)} \\ 0 & \text{(stage 2, 3)} \end{cases} \quad (29)$$

$$F_{\text{or}} = \begin{cases} 0 & \text{(stage 1)} \\ 2.6153\text{E} - 03 P_{\text{ps}}^{0.5563} + 22.18364 & \text{(stage 2, 3)} \end{cases} \quad (30)$$

$$F_{\text{ba}} = \begin{cases} 0 & \text{(stage 1, 3)} \\ 3000 & \text{(stage 2)} \end{cases} \quad (31)$$

where F_{or} and F_{ba} are, respectively, the friction force at the O-ring and the friction force by the balls. All other variables are explained in the Nomenclature.

To add redundancy, two initiators are connected in parallel. For the system to be successful, either one of the initiators must be operated. It is noted that the mean lengths of the two initiators are slightly different, as shown in Table 5, which reflects the effect of different environmental conditions. Therefore, it is expected that the probabilities of failure of the two initiators are different, as shown in Table 6. A failure of the both initiators leads to a malfunction of the PMD, which is undesirable. A DAG for this system is shown in Fig. 6. Denoting each initiator as I_1 and I_2 , the random variables used in the equations are listed in Table 5. All the random variables are assumed to follow a normal distribution, with 10% coefficient of variation. It is noted that there exists a model form uncertainty in the performance model, such as the shear-pin and O-ring forces. Therefore, it would be more practical if the confidence interval of system reliability includes the contribution from model form uncertainty, which would be the future plan for research.

B. Bayesian Network Formulation

A simple Bayesian network is built for this system, as shown in Fig. 6. To calculate P_F , a set of samples are generated based on the

Table 5 Random variables in PMD system

Random variables	Mean (I_1/I_2)	Random variables	Mean (I_1/I_2)
Initial temperature T_0	20°C	Heating element length l_e	41/40 mil
Heating element diameter d_e	2.3 mil	Conductivity κ	385 W/m · K
Emissivity ϵ	0.03	Length of pin l_{pin}	406 mil
Input current I	3.5 A	Charge density ρ_c	2440 kg/m ³
Mass of piston (m_{ps})	0.0152 kg	Mass of ball (m_{ba})	0.0696 kg
Ball friction F_{sh}	2500 N	Mass of charge (m_{gen})	20 mg
Shear pin force F_{sh}	233.9858 N	—	—

Table 6 Mean standard deviation estimation

Probability	Sample P_F^i	Mean ($\mu_{c,i}$)	Standard deviation ($\sigma_{c,i}$)
p_1	0.2	0.21	0.040
p_2	0.25	0.26	0.043
p_3	0.1	0.11	0.030
$p_4 (= p_3)$	0.1	0.11	0.030
$p_5 (= p_3)$	0.1	0.11	0.030
p_6	1.0	1.0	0.0

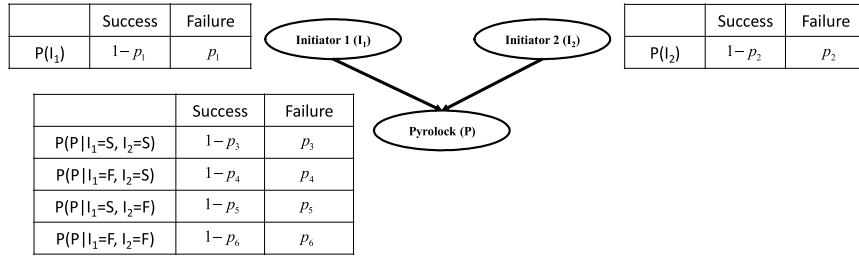


Fig. 6 Bayesian network of pyrotechnic mechanical device.

distributions given in Table 5. Then, these input samples are used to solve the differential equations in Eqs. (21–31), from which the success or failure of the component can be determined. This is equivalent to evaluating the indicator function in Eq. (2). This process is repeated n times to calculate P_F as in Eq. (1). For the two initiators, P_F is not conditional because they do not have any parent. On the other hand, P_F in the pyrolock is the conditional probability because its calculation depends on the success or failure of the initiators.

For this example, P_F is calculated using 100 samples randomly generated from each of the variables listed in Table 5 for the initiator and pyrolock. In the case of the initiators 1 and 2, exactly 20 and 25 of the 100 samples failed, respectively. When the initiator succeeds, 10 out of the 100 samples failed in the pyrolock. When both initiators fail, however, there is no chance to make the pyrolock work. Therefore, the corresponding conditional P_F is 100%; that is $p_6 = 1.0$. Moreover, the conditional P_F of the pyrolock would be the same if one or both initiators were a success; that is, $p_3 = p_4 = p_5$.

Based on these results, the mean and standard deviation of conditional P_F are estimated as shown in Table 6. For the standard deviation, the Wilson method in Table 1 has been used to make the most conservative estimate. It is noted that, for the given number of samples and the estimated conditional P_F , the sampling uncertainty in the pyrolock (p_3) is the lowest. Because of the difference in the heating element length of the two initiators, they are different by 25%.

In such a simple Bayesian network, the system P_F can be obtained using the following equation:

$$P_F^{sys} = p_1 p_2 - p_1 p_2 p_3 + p_3 \tag{32}$$

Then, the standard deviation of the system P_F is calculated as in Table 7, and the bounds of the SCI are obtained using Eq. (11) with the 95% confidence level. In such a simple network, it is obvious that the conditional P_F of the pyrolock will contribute the most for the system P_F . The other contribution is P_F due to the failure of the two initiators. It is also noted that the uncertainty in the system P_F is smaller than that of the two initiators but slightly larger than that of the pyrolock. The effect of large uncertainty in the two initiators is diminished when it goes through the network. Although conventional reliability methods can calculate the system reliability as well as its confidence intervals, this paper focuses on identifying the contribution of component-level reliability and confidence intervals to that of system. For this purpose, a Bayesian network provides a unique framework to facilitate the relationship between components and the system. In general, the methods of estimating the system probability of failure and its confidence intervals depend on the level

Table 7 System probability of failure and confidence interval

P_F^{sys}	σ_F^{sys}	Lower bound	Upper bound
0.15	0.031	0.084	0.206

Table 8 Sensitivity index

S_1	S_2	S_3	S_{12}	S_{13}	S_{23}	S_{123}
0.085	0.066	0.847	0.002	1E-04	7.7E-05	2.7E-06

Probability

Impossible	Wide Confidence Interval $(P_r, \epsilon_{P_r}) = (10^{-6}, 10^{-3})$ Bootstrap Wilson Exact
Wide Confidence Interval $(P_r, \epsilon_{P_r}) = (10^{-1}, 10^{-1})$ Bootstrap Wilson Exact	Narrow Confidence Interval $(P_r, \epsilon_{P_r}) = (10^{-1}, 10^{-5})$ Any method

Resources

Fig. 7 Possible method for different combinations of resource and probability.

of probability of failure and the amount of available resources, such as the number of samples. Figure 7 shows the recommended methods based on the level of probability and the amount of resources.

C. Global Sensitivity Analysis

The total sensitivity indices using ANOVA decomposition are obtained in the PMD system to identify the probability that influences the output variance the most. The decomposition is performed by substituting $h(P_F)$ in Eqs. (13) and (14) with Eq. (32). There are seven sensitivity indices for this example. Using the decomposed functions, the total sensitivity indices are calculated in Table 8. Even though the standard deviation of p_3 was the smallest, as shown in Table 6, the corresponding total sensitivity index is the highest. Thus, the variance of the system is mainly due to p_3 , and therefore it is necessary to provide more samples to p_3 to efficiently reduce the system variance.

This result can be explained based on the shape of the network. Because the pyrolock is the end of the network, its CCI directly affects the SCI. On the other hand, the effect of the initiators' CCI is diminished when it goes through the network. Therefore, the most effective way of reducing the SCI is to reduce the CCI of the closest component to the system. In practical systems, however, tests tend to be more expensive toward the system level. Therefore, adding samples at different components may cause different costs. Therefore, the global sensitivity analysis has to be interpreted in conjunction with the cost model of reducing sampling uncertainty.

VI. Conclusions

In this paper, four different interval methods and nonparametric bootstrap method were used to establish a confidence interval of components as well as the system in a Bayesian network. For a midrange probability, all five methods showed a wider confidence interval than the true one. If the most conservative decision is to be made, then the Wilson method should be used because it showed the widest confidence interval when the same number of samples are employed.

A numerical example showed that the confidence interval is highly dependent on the number of initial samples, not on the number of bootstrap repetitions. However, a high enough number of bootstrap

repetitions must be used, although how many is enough is to be discussed in future research.

Out of four interval methods, the Wilson and Clopper–Pearson methods succeeded to yield a reasonable confidence interval for an extreme level of P_F (97–99.9%), in which the upper bound does not go beyond 1. The bootstrap method always gives a confidence interval within the bound of a probability definition (0 to 1) because the method is based on resampling.

Global sensitivity analysis using ANOVA decomposition works well to resolve the resource allocation problem. As shown in Sec. V, the highest variance does not guarantee the highest total sensitivity index. Therefore, the global sensitivity analysis must be adopted to efficiently reduce the confidence interval width.

Also, the four interval methods has been speculated considering the target probability and available resources. If the target probability is extreme and resource is insufficient, then there is no way to obtain a reasonable confidence interval. If the situation reverses (i.e., when a confidence interval is pursued a midrange target probability using the abundant resource), then any method listed in Sec. II will work. When the target probability is extreme and the resource is ample or the target probability is not extreme but still the resource is insufficient, bootstrap, Wilson, or Clopper–Pearson method will work. Wald and adjusted Wald method may not work because of the normality condition.

Acknowledgment

This research was also supported by the research grant (PMD) of the Agency for Defense Development and Defense Acquisition Program Administration of the Korean Government.

References

- [1] Pukite, J., and Pukite, P., *Modeling for Reliability Analysis: Markov Modeling for Reliability, Maintainability, Safety, and Supportability Analyses of Complex Systems*, Wiley, New York, 1998, pp. 35–47.
- [2] Holmes, D. E., and Jain, L. C. (eds.), *Innovations in Bayesian Networks: Theory and Applications*, Springer–Verlag, Berlin, 2008, pp. 221–227.
- [3] Sankararaman, S., McLemore, K., Mahadevan, S., Bradford, S. C., and Peterson, L. D., “Test Resource Allocation in Hierarchical Systems Using Bayesian Networks,” *AIAA Journal*, Vol. 51, No. 3, 2013, pp. 537–550.
doi:10.2514/1.J051542
- [4] Price, N. B., Kim, N.-H., Haftka, R. T., Balesdent, M., Defoort, S., and Le Riche, R., “Deciding Degree of Conservativeness in Initial Design Considering Risk of Future Redesign,” *Journal of Mechanical Design*, Vol. 138, No. 11, Nov. 2016, Paper 111409.
doi:10.1115/1.4034347
- [5] Coit, D. W., “System-Reliability Confidence-Intervals for Complex-Systems with Estimated Component-Reliability,” *IEEE Transactions on Reliability*, Vol. 46, No. 4, Dec. 1997, pp. 487–493.
doi:10.1109/24.693781
- [6] Levy, L. L., and Moore, A. H., “A Monte Carlo Technique for Obtaining System Reliability Confidence Limits from Component Test Data,” *IEEE Transactions on Reliability*, Vol. 15, No. 2, Sept. 1967, pp. 69–72.
doi:10.1109/TR.1967.5217462
- [7] Cruse, T. A., Mahadevan, S., Huang, Q., and Mehta, S., “Mechanical System Reliability and Risk Assessment,” *AIAA Journal*, Vol. 32, No. 11, 1994, pp. 2249–2259.
doi:10.2514/3.12284
- [8] Mahadevan, S., Zhang, R., and Smith, N., “Bayesian Networks for System Reliability Reassessment,” *Structural Safety*, Vol. 23, No. 3, 2001, pp. 231–251.
doi:10.1016/S0167-4730(01)00017-0
- [9] Cheng, J., and Druzzzel, M. J., “Confidence Inference in Bayesian Networks,” *Proceedings of the Annual Conference on Uncertainty in Artificial Intelligence (UAI-2001)*, Morgan Kaufmann, San Francisco, 2001, pp. 75–82.
- [10] Jensen, F. V., and Nielsen, T. D., *Bayesian Networks and Decision Graphs*, Springer, New York, 2007, pp. 32–42.
- [11] Ramsey, M. H., “Sampling as a Source of Measurement Uncertainty: Techniques for Quantification and Comparison with Analytical Sources,” *Journal of Analytical Atomic Spectrometry*, Vol. 13, No. 2, 1998, pp. 97–104.
doi:10.1039/a706815h
- [12] Fraser, D. A. S., *Statistics: An Introduction*, Wiley, Hoboken, NJ, 1958, Chap. 2.
- [13] Brown, L. D., Cai, T. T., and DasGupta, A., “Interval Estimation for a Binomial Proportion,” *Statistical Science*, Vol. 16, No. 2, 2001, pp. 101–133.
- [14] Wallis, S., “Binomial Confidence Intervals and Contingency Tests: Mathematical Fundamentals and the Evaluation of Alternative Methods,” *Journal of Quantitative Linguistics*, Vol. 20, No. 3, 2013, pp. 178–208.
doi:10.1080/09296174.2013.799918
- [15] Wilson, E. B., “Probable Inference, the Law of Succession, and Statistical Inference,” *Journal of the American Statistical Association*, Vol. 22, No. 158, June 1927, pp. 209–212.
doi:10.1080/01621459.1927.10502953
- [16] Clopper, C. J., and Pearson, E. S., “The Use of Confidence or Fiducial Limits Illustrated in the Case of the Binomial,” *Biometrika*, Vol. 26, No. 4, Dec. 1934, pp. 404–413.
doi:10.1093/biomet/26.4.404
- [17] Thulin, M., “The Cost of Using Exact Confidence Intervals for a Binomial Proportion,” *Electronic Journal of Statistics*, Vol. 8, No. 1, 2014, pp. 817–840.
doi:10.1214/14-EJS909
- [18] Sauro, J., and Lewis, J. R., “Estimating Completion Rates from Small Samples Using Binomial Confidence Intervals: Comparisons and Recommendations,” *Proceedings of the Human Factors and Ergonomics Society*, Vol. 49, No. 24, Sept. 2005, pp. 2100–2103.
- [19] Li, C., and Mahadevan, S., “Role of Calibration, Validation, and Relevance in Multi-Level Uncertainty Integration,” *Reliability Engineering and System Safety*, Vol. 148, April 2016, pp. 32–43.
doi:10.1016/j.res.2015.11.013
- [20] Picheny, V., Kim, N. H., and Haftka, R. T., “Application of Bootstrap Method in Conservative Estimation of Reliability with Limited Samples,” *Structural and Multidisciplinary Optimization*, Vol. 41, No. 2, March 2010, pp. 205–217.
doi:10.1007/s00158-009-0419-8
- [21] Tu, J., and Choi, K. K., “A New Study on Reliability Based Design Optimization,” *ASME Journal of Mechanical Design*, Vol. 121, No. 4, 1999, pp. 557–564.
doi:10.1115/1.2829499
- [22] Rangavajhala, S., Liang, C., and Mahadevan, S., “Design Optimization Under Aleatory and Epistemic Uncertainties,” *12th AIAA Aviation Technology, Integration, and Operations Conference*, AIAA Paper 2012-5665, Sept. 2012.
- [23] Jiang, Z., Chen, W., and German, B. J., “Multidisciplinary Statistical Sensitivity Analysis Considering Both Aleatory and Epistemic Uncertainties,” *AIAA Journal*, Vol. 54, No. 4, 2016, pp. 1326–1338.
doi:10.2514/1.J054464
- [24] Saltelli, A., “Global Sensitivity Analysis: An Introduction,” *Proceedings of the 4th International Conference on Sensitivity Analysis of Model Output (SAMO'04)*, March 2004, pp. 27–43.
- [25] Jang, S. G., Lee, H. N., and Oh, J. Y., “Performance Modeling of a Pyrotechnically Actuated Pin Puller,” *International Journal of Aeronautical & Space Science*, Vol. 15, No. 1, 2014, pp. 102–111.
doi:10.5139/IJASS.2014.15.1.102
- [26] Hwang, D., Lee, J., Han, J.-H., Lee, Y., and Kim, D., “Numerical Analysis and Simplified Mathematical Modeling of Separation Mechanism for the Ball-Type Separation Bolt,” *Proceedings of the Korean Society of Propulsion Engineers*, Aug. 2015, pp. 1–8.

R. Ghanem
Associate Editor